

Comparative Molecular Similarity Indices Analysis of Caspase-3 Inhibitors

Sathya Babu and Thirumurthy Madhavan[†]

Abstract

Caspases, a family of cysteinyl aspartate-specific proteases plays a central role in the regulation and the execution of apoptotic cell death. Activation of caspases-3 stimulates a signaling pathway that ultimately leads to the death of the cell. Hence, caspase-3 has been proven to be an effective target for reducing the amount of cellular and tissue damage. In this work, comparative molecular similarity indices analysis (CoMSIA) was performed on a series of 3,4-dihydropyrimidoindolones derivatives which are inhibitors of caspase-3. The best predictions were obtained for CoMSIA model ($q^2 = 0.586$, $r^2 = 0.955$). The predictive ability of test set (r^2_{pred}) was 0.723. Statistical parameters from the generated QSAR models indicated the data is well fitted and have high predictive ability. Our theoretical results could be useful to design novel and more potent caspase-3 derivatives.

Key words: Caspase-3, CoMSIA

1. Introduction

Caspases, a family of cysteinyl aspartate-specific proteases which mediates the signaling pathway and plays a central role in the regulation and the execution of apoptotic cell death^[1-4]. Caspases are synthesized as zymogens (pro-caspase) which are activated by various triggers and cause the active caspase to express itself and carry out specific function. It cleaves target proteins at specific aspartate residues^[5]. Caspases are essential effector molecules for carrying out apoptosis in eukaryotic cells^[4]. Till now 11 known human caspases has been discovered and which can be divided into three sub-types based on their structure and function^[3]. Group I caspases (1, 4, 5 and 14) are primarily involved in inflammation. Group II caspases (6, 8, 9 and 10) are primary involved in apoptosis as upstream regulators of the Group III caspases (3 and 7). The Group III caspases are effector caspases that, once activated, stimulate a signaling pathway that ultimately leads to the death of the cell^[6]. Failure of apoptosis is one of the main contributions to tumour development, central

nervous diseases and autoimmune diseases; this coupled with unwanted apoptosis that occurs with ischemia or Alzheimer's disease, has stimulated interest in caspases as potential therapeutic targets for drug development^[7].

Recent study has shown that caspase inhibition can help in tissue protection^[8-12]. The basic structural feature of almost all known caspase inhibitors is an electrophilic group that lead to inactivation of the enzyme by forming reversible or irreversible bond with the active site cysteine^[13]. Caspases-3 is common to all currently known caspases^[6,14] and plays a key role in apoptosis among several different groups of caspase enzymes^[15]. Many groups have been reported their efforts toward selective, small molecule caspase-3 inhibitors^[16-19]. Caspase-3 has been proven to be an effective target for reducing the amount of cellular and tissue damage in cell culture and animal models by specific inhibitors^[10,11]. Till to date, many studies have been published in which the combination of 2D and 3D-QSAR techniques have proven the successful role in the modern drug discovery process^[20]. We formulate a reasonable 3D-QSAR model based on ligand alignment. Our study thoroughly discussed the CoMSIA models for a set of caspase-3 inhibitors and emphasized the significant parameters for higher activity. Our optimum QSAR models could be a good starting point for ligand optimization and guidance for medicinal chemist to

Department of Bioinformatics, School of Bioengineering, SRM University, SRM Nagar, Kattankulathur, Chennai 603203, India

[†]Corresponding author : thiru.murthyunom@gmail.com,
thirumurthy.m@ktr.srmuniv.ac.in

(Received : November 13, 2014, Revised : December 15, 2014,
Accepted : December 25, 2014)

derive future non-peptidic inhibitors of caspase-3 derivatives.

2. Computational Details

2.1. Dataset

A series 35 compounds has been taken from the literature with their biological activities in terms of IC_{50} values^[19]. These are identified as lead series of novel 3,4-dihydropyrimidoindolones and considered as potent and selective inhibitors of caspase-3. The binding affinities of given pyrimidoindolones concentration in nano molar (nM) range were converted to the molar (M) concentration and then converted to logarithmic scale for further QSAR analyses on dataset, using the following formula.

$$pIC_{50} = -\log (IC_{50}).$$

Total dataset is divided randomly into a training set of 27 compounds and test set (wide range of activity) of 8 compounds which has been shown in Table 1.

2.2. Molecular Modeling

All computational studies were performed using molecular modeling package SYBYL 8.1 installed on a Linux system. The initial step is to find out the most active molecule within the dataset. Random search method has been done to derive the least energy conformation which is considered as a bioactive conformation and it is then minimized by applying Tripos force field. Finally Gasteiger- Hückel charges were applied to all the molecules of dataset and it was subsequently used for QSAR studies. As compound 31 was the most active, all the possible conformations were obtained by systematic conformational analysis and the lowest energy conformer was assumed as bioactive conformer and was chosen for subsequent QSAR modeling. Using this particular conformer structure as standard, bioactive conformations for other compounds were determined by systematic conformer search for the additional moieties, by keeping core part constrained. In this way, the common scaffold of every inhibitor occupies the same area in three-dimensional space.

Table 1. Structures and biological activities (pIC_{50}) of caspase-3 inhibitors

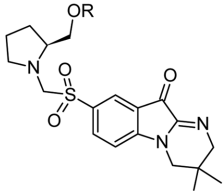
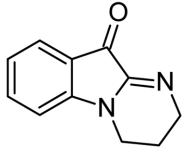
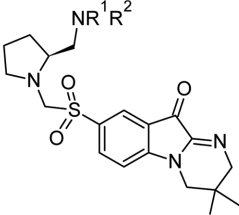
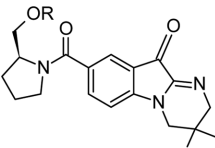
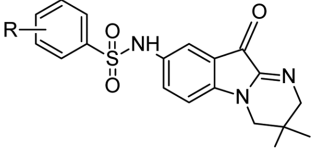
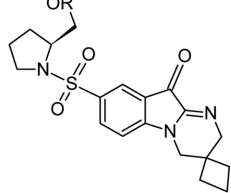
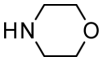
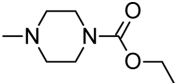

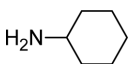
				
Compound 1-15	General Structure	Compound 16-19		
				
Compound 20-21	Compound 22-29	Compound 30-35		
Compound	R	NR ¹ R ²	n	pIC_{50}
1	Phenyl	-	-	8.155
2	4-F-phenyl	-	-	7.968
3	4-OCH ₃ -phenyl	-	-	7.859
4*	4-Cl phenyl	-	-	7.432
5	4-Ac phenyl	-	-	7.523

Table 1. Continued

Compound	R	NR ¹ R ²	n	pIC ₅₀
6*	4-t-Bu phenyl	-	-	7.092
7	4-F-3-CH ₃ phenyl	-	-	7.638
8	4-OCH ₃ -2-Cl phenyl	-	-	7.086
9	2-Pyridyl	-	-	8.107
10*	5-Cl 2-pyridyl	-	-	7.990
11	6-CH ₃ 2-pyridyl	-	-	7.901
12	3-pyridyl	-	-	8.620
13	5-Cl 3-pyridyl	-	-	8.354
14*	2-CH ₃ 3-pyridyl	-	-	8.144
15	5-CO ₂ CH ₃ 3-pyridyl	-	-	7.994
16	-		-	8.302
17	-		-	7.844
18*	-		-	7.360
19	-		-	7.229
20*	Ph	-	-	4.301
21	CH ₃	-	-	6.000
22	H	-	-	6.439
23*	2-F	-	-	6.830
24	3-CF ₃	-	-	6.719
25	3-OCH ₃	-	-	6.456
26	4-Cl	-	-	5.874
27	4-OCH ₃	-	-	5.823
28*	4-OCF ₃	-	-	5.598
29	4-F	-	-	5.621
30	CH ₃	-	1	8.481
31	Ph	-	1	8.889
32	CH ₃	-	2	7.829
33	Ph	-	2	8.365
34	CH ₃	-	3	7.866
35	Ph	-	3	7.609

*Test set compounds

2.3. Alignment Method

The accuracy and reliability of the CoMSIA is directly dependent on the structural alignment rule^[21]. Structural alignment is the most subjective and critical rule in QSAR studies. The quality of ligand alignment plays very essential role. The use of low energy conformation in the alignment is the useful starting

point for statistical comparisons of flexible structures within CoMSIA models. Conformational energies were computed with electrostatic term, and the lowest energy conformer was selected as template molecule. The most active molecule was used as the reference to align all the compounds using atom-to-atom matching. The minimized structures were aligned over the template

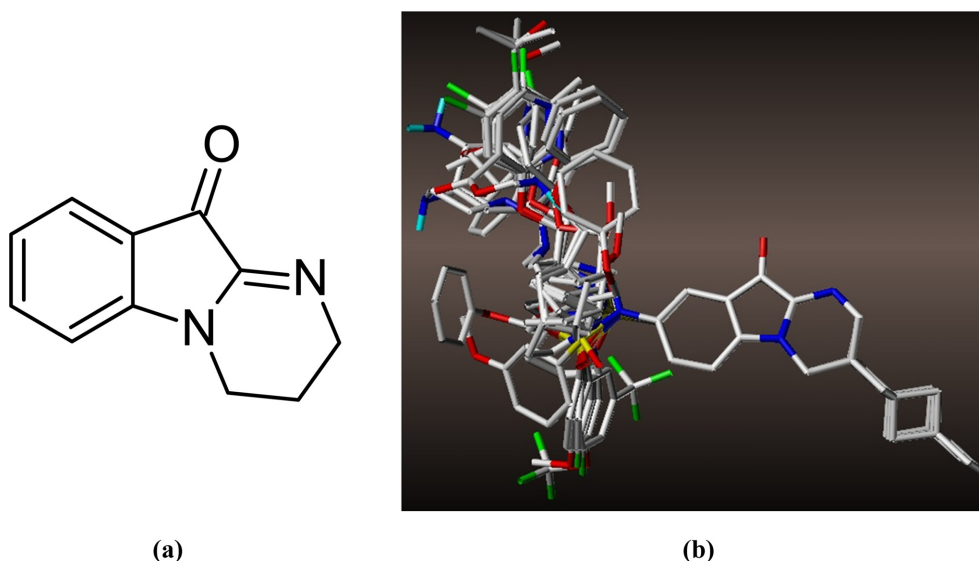


Fig. 1. (a) Maximum common substructure for atom by atom matching, (b) Superimposed structures after optimization with Gasteiger-Huckel charge.

using the atom fit option in Sybyl, and subsequently, this alignment was used for CoMSIA analysis. The matching atoms were selected by maximum common substructure (MCS) as shown in Fig. 1(a) and the alignment of the all the molecules are represented in Fig. 1(b).

2.4. CoMSIA Model Generation

In CoMSIA studies, the molecular similarity was expressed in terms of five different properties: steric, electrostatic, hydrophobic, hydrogen (H)-bond donor, and H-bond acceptor. The properties were calculated using a C+ probe atom with a radius of 1 Å placed at a regular grid spacing of 2 Å. CoMSIA similarity indices ($A_{F,k}^q$) for molecule j with atom i at a grid point q were calculated using the equation 1.

$$A_{F,k}^q(j) = -\sum \omega_{prob,k} \omega_{ik} e^{-\alpha r^2} i q \quad (1)$$

where k represents the following physicochemical properties: steric, electrostatic, hydrophobic, H-bond donor, and H-bond acceptor. A Gaussian type distance dependence was used between grid point q and each atom i of the molecule. The default value of 0.3 was used as the attenuation factor (α). The steric indices were related to the third power of the atomic radii; electrostatic descriptors were derived from atomic partial charges; hydro-

phobic fields were derived using atom-based parameters and H-bond donor and acceptor indices were obtained by a rule-based method based on experimental results^[22]. With standard option for the scaling of variables, the regression analysis was carried out using cross-validated partial least squares approach (PLS) of LOO (leave-one-out)^[23]. After the optimal number of components was determined, a non-cross-validated analysis was carried out without column filtering.

2.5. Partial Least Squares (PLS) Analysis

In 3D-QSAR, the CoMSIA descriptors were used as independent variables and pIC50 values were used as the dependent variable. The PLS method was used to linearly correlate these CoMSIA descriptors with the biological activity values. All fields were scaled by the default options in SYBYL. Cross-validation analysis was performed using the LOO method. The cross-validated correlation coefficient (q^2) that resulted in optimum number of components and lowest standard error of prediction were considered for further analysis.

3. Results and Discussion

In the present work, we have applied CoMSIA on a set of non-peptidic inhibitors derivatives to build 3D-QSAR models. During model generation, we have

formulated different strategies in order to derive statistically robust QSAR model. The best predictions were obtained for CoMSIA model ($q^2=0.586$, $r^2=0.955$). Finally, the obtained value was used for further analysis in order to generate CoMSIA steric, electrostatic, hydrophobic, H-bond donor and acceptor contour plots.

3.1. CoMSIA Model Analysis

In this the compounds were divided into training and test set where the training set was used to construct the model and test set was used to validate the model. Different field combinations of CoMSIA models were generated using Gasteiger-Hückel charge method with 2.0 Å grid space. The combinations of all descriptors such as steric (S), electrostatic (E), hydrophobic (H),

hydrogen bond donor (D), and hydrogen bond acceptor (A) were listed in Table 2. The optimum model for CoMSIA analysis was selected based on higher q^2 , r^2 and r^2_{pred} values. The optimum CoMSIA model was obtained with the combination of S, and H parameters. The final model for CoMSIA yielded $q^2=0.586$ and $r^2=0.955$ with $N=4$. The percentage field contributions value showed that E (37.3%) and D (62.7%) fields contributing more for the model development. The SEE for CoMSIA model was found to be 0.212 and F value was 117.656. The predictive ability of the developed CoMSIA model was assessed by the test set (five molecules) predictions, which were excluded during CoMSIA model generation. The predictive ability of the test set was 0.723.

Table 2. Ligand based statistical results of CoMSIA models

No	Field contribution					LOO cross-validation		Non-cross-validation			r^2_{pred}
	S	E	H	D	A	q^2	N	r^2	SEE	F	
Ligand-based alignment											
1	0.505	0.495	-	-	-	0.617	1	0.709	0.506	61.009	-
2	-	0.415	0.585	-	-	0.590	1	0.707	0.509	60.215	-
3	-	-	0.936	0.064	-	0.547	3	0.834	0.399	38.597	-
4	-	-	-	0.128	0.872	0.635	2	0.748	0.482	35.554	-
5	0.373	-	0.627	-	-	0.586	4	0.955	0.212	117.656	0.723
6	0.873	-	-	0.127	-	0.616	2	0.727	0.501	31.999	-
7	0.466	-	-	-	0.534	0.638	1	0.718	0.499	63.522	-
8	-	0.884	-	0.116	-	0.616	2	0.732	0.496	32.837	-
9	-	0.462	-	-	0.538	0.641	1	0.727	0.491	66.536	-
10	0.297	0.292	0.411	-	-	0.602	1	0.708	0.508	60.553	-
11	0.327	0.314	-	-	0.366	0.637	1	0.721	0.496	64.692	-
12	0.446	0.437	-	0.117	-	0.629	2	0.739	0.490	33.987	-
13	-	0.280	0.394	-	0.326	0.626	1	0.722	0.495	65.031	-
14	-	0.382	0.530	0.087	-	0.595	2	0.734	0.495	33.050	-
15	0.284	-	0.392	-	0.324	0.623	1	0.714	0.503	62.290	-
16	0.360	-	0.574	0.066	-	0.589	4	0.921	0.282	63.793	-
17	-	0.336	-	0.272	0.392	0.637	1	0.689	0.524	55.415	-
18	0.274	0.270	0.375	0.081	-	0.605	2	0.742	0.487	34.491	-
19	0.222	0.218	0.307	-	0.254	0.625	1	0.719	0.498	63.914	-
20	0.255	0.251	-	0.203	0.292	0.635	1	0.730	0.488	67.76	-
21	-	0.228	0.321	0.185	0.266	0.625	1	0.726	0.492	66.267	-
22	0.232	-	0.320	0.184	0.265	0.620	1	0.720	0.497	64.372	-
24	0.189	0.185	0.261	0.150	0.216	0.624	1	0.737	0.482	70.114	-

S= steric; E= electrostatic; H= hydrophobic; D= hydrogen bond donor; A= hydrogen bond acceptor q^2 = cross-validated correlation coefficient; N= number of statistical components; r^2 = non-cross validated correlation coefficient; SEE=standard estimated error; F=Fisher value; $r^2_{predictive}$ = predictive correlation coefficient for test set.

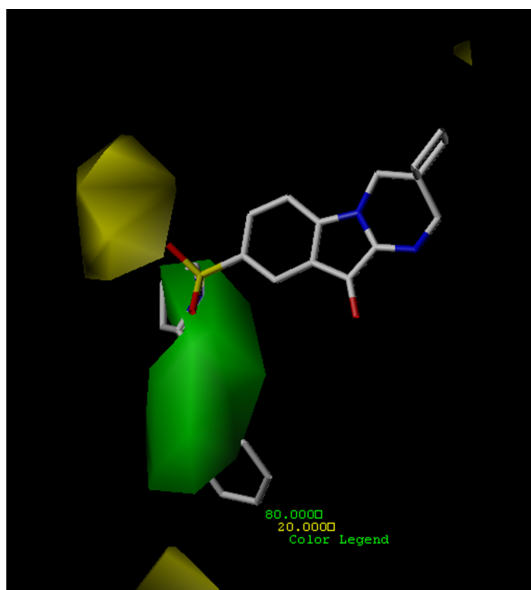


Fig. 2. CoMFA contour maps for steric field with highly active compound 31, where green contour indicates regions where bulky groups increases activity and yellow contours indicates bulky groups decreases activity.

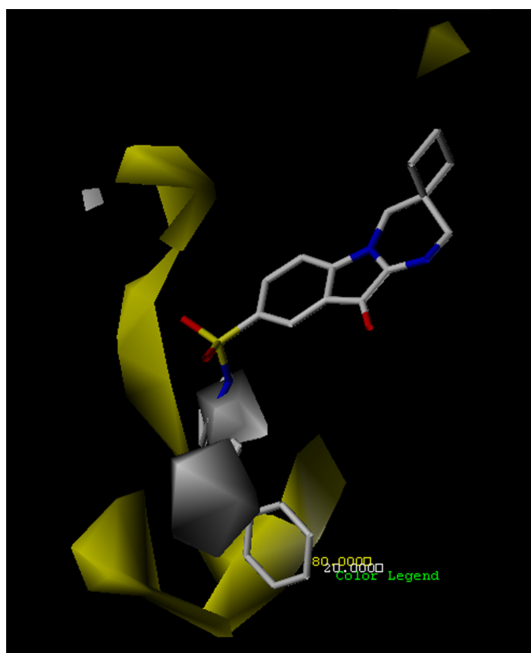


Fig. 3. CoMFA contour maps for hydrophobic field with highly active compound 31, where yellow contour map indicates the region where the hydrophobic substitutions are favourable for activity and white contour indicates the disfavored region for inhibitory activity.

As we know the PLS QSAR model was used not only to predict the data but also the contour map. The contour map of steric fields is shown in Fig. 2. The steric contour map was shown with green (favoured level 80%) and yellow (disfavoured level 20%). The contour map of hydrophobic fields is shown in Fig. 3. The hydrophobic contour map was shown with yellow (favoured level, 80%) and white (disfavoured level 20%). The higher activity is correlated with more bulk near green and larger hydrophobicity in the yellow and vice versa. The presence of bulky substituent at R position in the 5 membered ring attached to the sulphur atom increases activity. For example in the highly active compound 31 the R position has phenyl ring attached to the 5 membered ring which is attached to sulphur atom and second highly active compound 33 also has the phenyl ring attached the R position. Presence of bulky group at R without sulphur atom has decreased activity in the compound 20. Hence the bulky group at R position of 5 membered ring attached to the sulphur atom is responsible for increasing activity in 3,4-dihydropyrimidindolones derivatives of caspase 3 inhibitors.

4. Conclusion

In the present study, we developed satisfactory 3D-QSAR models of 3,4 dihydropyrimidindolones derivatives using CoMSIA based on the atom-by-atom matching alignment. We have been formulated different strategies in order to derive statistically robust 3D-QSAR models. The CoMSIA model constructed with steric and hydrophobic fields show good predictive ability and revealed some important sites, where steric and hydrophobic modifications could significantly affect the bioactivities of the compounds. The information's have gathered from CoMSIA studies demonstrated the way to understand the structural and chemical features in designing and finding new potential caspase-3 inhibitors.

References

- [1] M. D. Jacobson, M. Weil, and M. C Raff, "Programmed cell death in animal development", *Cell*, Vol. 88, pp. 347-354, 1997.
- [2] G. M. Cohen, "Caspases: the executioners of apoptosis", *J. Biochem.*, Vol. 326, pp. 1-16, 1997.
- [3] C. B. Thonberry and Y. Lazebnik, "Caspases: ene-

- mied within”, *Science*, Vol. 281, pp. 1312-1316, 1998.
- [4] D. W. Nicolson, “Caspase structure, proteolytic substrates, and function during apoptotic cell death”, *Cell Death Differ.*, Vol. 6, pp. 1028-1042, 1999.
- [5] J. Wang and M. J. Lenardo, “Roles of caspases in apoptosis, development and cytokine maturation revealed by homozygous gene deficiencies”, *J. Cell Sci.*, Vol. 113, pp. 753-757, 2000.
- [6] M. Endres, S. Namura, M. Shomizu-Sasamata, C. Waeber, L. Zhang, T. Gomez-Isla, B. T. Hyman, and M. A. Moskowitz, “Attenuation of delayed neuronal death after mild focal ischemia in mice by inhibition of caspase family”, *J. Cerebr. Blood F. Met.*, Vol. 18, pp. 238-247, 1998.
- [7] K. M. Boatright and G. S. Salvesen, “Mechanisms of caspase activation”, *Curr. Opin. Cell Biol.*, Vol. 15, pp. 725-731, 2003.
- [8] B. A. Callus and D. L. Vaux, “Caspase inhibitors: viral, cellular and chemical”, *Cell Death Differ.*, Vol. 14, pp. 73-78, 2007.
- [9] B. R. Hu, C. L. Liu, Y. Ouyang, K. Blomgren, and B. K. Siesjo, “Involvement of caspase-3 in cell death after hypoxischemia declines during brain maturation”, *J. Cerebr. Blood F. Met.*, Vol. 20, pp. 1294-1300, 2002.
- [10] R. S. Hotchkiss, K. C. Chang, P. E. Swanson, K. W. Tinsley, J. J. Hui, P. Klender, S. Xanthoudakis, S. Roy, C. Black, E. Grimm, R. Aspiotis, Y. Han, D. W. Nicholson, and I. E. Karl, “Caspase inhibitors improves survival in sepsis: a critical role of the lymphocyte”, *Nat. Immunol.*, Vol.1, pp. 496-501, 2000.
- [11] D. Lee, S. A. Long, J. H. Murray, J. L. Adams, M. E. Nuttall, D. P. Nadeau, K. Kikly, J. D. Winkler, C.-M. Sung, M. D. Ryan, M. A. Levy, P. M. Keller, and W. E. DeWolf, Jr., “Potent and selective non peptide inhibitors of caspase 3 and 7”, *J. Med. Chem.*, Vol. 44, pp. 2015-2026, 2001.
- [12] H. Yaoita, K. Ogawa, K. Maehara, and Y. Maruyama, “Attenuation of ischemia/reperfusion injury in rats by a caspase inhibitor”, *Circulation*, Vol. 97, pp. 276-281, 1998.
- [13] J. Schoenberger, J. Bauer, J. Moosbauer, C. Eilles, and D. Grimm, “Innovative strategies in in-vivo apoptosis imaging”, *Curr. Med. Chem.*, Vol. 15, pp. 187-194, 2008.
- [14] D. K. Perry, M. J. Smyth, H. R. Stennicke, G. S. Salvessan, P. Duriez, G. G. Poirier, and Y. A. Hannun, “Zinc is a potent inhibitor of the apoptotic protease, caspase-3. A novel target for zinc in the inhibition of apoptosis”, *J. Biol. Chem.*, Vol. 272, pp. 18530-18533, 1997.
- [15] G. Porter and R. U. Janicke, “Emerging roles of caspase 3 in apoptosis”, *Cell Death Differ.*, Vol. 6, pp. 99-104, 1999.
- [16] C. W. Scott, C. Sobotka-Brinker, D. E. Wilkins, R. T. Jacobs, J. J. Folmer, W. J. Frazee, R. V. Bhat, S. V. Ghanekar, and D. Aharony, “Novel small molecule inhibitors of caspase-3 block cellular and biochemical features of apoptosis”, *J. Pharmacol. Exp. Ther.*, Vol 304, pp. 433-440, 2003.
- [17] D. V. Kravchenko, V. M. Kysil, S. E. Tkachenko, S. Maliarchouk, I. M. Okun, and A. V. Ivanchtchenko, “Pyrrolo[3,4-c]quinoline-1,3-diones as potent caspase-3 inhibitors. Synthesis and SAR of 2-substituted 4-methyl-8-(morpholine-4-sulfonyl)-pyrrolo [3,4-c]quinoline-1,3-diones”, *Eur. J. Med. Chem.*, Vol. 40, pp. 1377-1383, 2005.
- [18] W. Chu, J. Zhang, C. Zeng, J. Rothfuss, Z. Tu, Y. Chu, D.E. Reichert, M. J. Welch, and R. H. Mach, “N-Benzylisatin sulfonamide analogues as potent caspase-3 inhibitors: Synthesis, in vitro activity and molecular modeling studies”, *J. Med. Chem.*, Vol. 48, pp. 7637-7647, 2005.
- [19] L. M. Havran, D. C. Chong, W. E. Childers, P. J. Dollings, A. Dietrich, B. L. Harrison, V. Marathias, G. Tawa, A. Aulabaugh, R. Cowling, B. Kapoor, W. Xu, L. Mosyak, F. Moy, W.-T. Hum, A. Wood, and A. J. Robichaud, “3,4-Dihydropyrimido (1, 2-a) indol-10 (2H)-ones as potent non-peptidic inhibitors of caspase-3”, *Bioorgan. Med. Chem.*, Vol. 17, pp. 7755-7768, 2009.
- [20] M. Thirumurthy, K. Gagan, G. Changdev, and J. C. Segung, “QSAR analysis on PifPK7 inhibitors using HQSAR, CoMFA and CoMSIA”, *Medicinal Chemistry Research*, Vol. 21, pp. 681-693, 2012.
- [21] S. J. Cho and A. Tropsha, “Cross validated R2 guided region selection for comparative molecular field analysis: a simple method to achieve consistent results”, *J. Med. Chem.*, Vol. 38, pp. 1060-1066, 1995
- [22] G. Klebe, U. Abraham, and T. Mietzner, “Molecular similarity indices in a comparative analysis (CoMSIA) of drug molecules to correlate and predict their biological activity”, *J. Med. Chem.*, Vol. 37, pp. 4130-4146, 1994.
- [23] S. Wold, M. Sjostrom, and L. Eriksson, “PLS regression: a basic tool of chemometrics”, *Chemometr. Intell. Lab.*, Vol. 58, pp. 109-130, 2001.